COMPARISON OF DIFFERENT SIMULATION CODES WITH UNILAC MEASUREMENTS FOR HIGH BEAM CURRENTS

L. Groening, W. Barth, W. Bayer, G. Clemente, L. Dahl, P. Forck, P. Gerhard,
I. Hofmann, M.S. Kaiser, M. Maier, S. Mickat, T. Milosic, G. Riehl, H. Vormann,
S. Yaramyshev, GSI, D-64291 Darmstadt, Germany
D. Jeon, SNS, ORNL, Oak Ridge, TN 37831, USA
D. Uriot, CEA IRFU, F-91191 Gif-sur-Yvette, France
R. Tiede, Goethe University, Frankfurt a.M., Germany

Abstract

The GSI Univeral Linear Accelerator UNILAC can accelerate all ion species from protons to uranium. Hence its DTL section is equipped with e.m. quadupoles allowing for a wide range of field strength along the section. During the last years various campaigns on the quality of high current beams at the DTL exit as a function of the applied transverse focusing have been performed. Measurements were compared with up to four different high intensity beam dynamics codes. Those comparisons triggered significant improvement of the final beam quality. The codes were used to prepare an ambitious and successful beam experiment on the first observation of a space charge driven octupolar resonance in a linear accelerator.

INTRODUCTION

In the last decades many beam dynamics computer codes were developed [1] in order to simulate emittance growth along a linac. Several benchmarking studies among codes have been performed [2, 3, 4] generally assuming idealized conditions as initial Gaussian distributions, equal transverse emittances, matched injection into a periodic lattice, and small longitudinal emittance with respect to the rf-bucket size. In case of an operating linac generally not all of these conditions are met. To apply simulation codes to a realistic environment a benchmark activity was started aiming at simulations of beam emittance measurements performed at a DTL entrance and exit, respectively. The studies were performed at the GSI UNILAC [5]. For the simulations four different codes were used: DYNAMION [6], PARMILA [7], TraceWin [8], and LORASR [9].

The first benchmarking was done with moderate mismatch with respect to the periodic DTL solution. The zero current transverse phase advance σ_o has been varied from 35° to 90°. A detailed description of this first campaign is given in [10]. A second campaign suggested in [11] aimed at exploration of the 90° stop-band by varying σ_o from 60° to 130°. In this campaign the mismatch was minimized in order to mitigate the effects of the envelope instability. Ref. [12] is dedicated to this campaign.

EXPERIMENT SET-UP AND PROCEDURE

Intense beams are provided by a MUCIS source at low charge states with the energy of 2.2 keV/u. An RFQ followed by two IH-cavities (HSI section) accelerates the ions to 1.4 MeV/u using an rf-frequency of 36 MHz. A subsequent gas-stripper increases the average charge state of the ion beam. Final acceleration to 11.4 MeV/u is done in the Alvarez DTL section operated at 108 MHz. The increase of rf-frequency by a factor of three requires a dedicated matching section preceding the DTL. It comprises a 36 MHz re-buncher for longitudinal bunch compression, a 108 MHz re-buncher for final bunch rotation, a quadrupole doublet for transverse compression, and a quadrupole triplet for final transverse beam matching.

The Alvarez DTL comprises five independent rf-tanks. Transverse beam focusing is performed by quadrupoles in the F-D-D-F mode. Each drift tube houses one quadrupole. The periodicity of the lattice is interrupted by four inter-tank sections, where D-F-D focusing is applied. Acceleration is done -30° from crest in the first three tanks and -25° from crest in the last two tanks.

Figure 1 presents the schematic set-up of the experiments. Beam current transformers are placed in front of

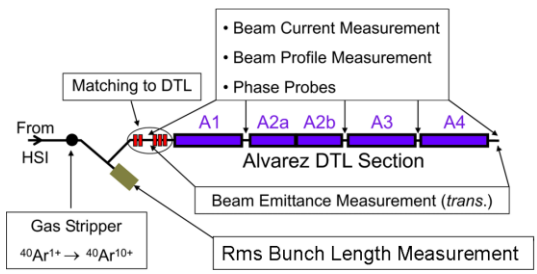

Figure 1: Schematic set-up of the experiments.

and behind the DTL as well as horizontal and vertical slit/grid emittance measurement devices. The total accuracy of each rms emittance measurement including its evaluation is estimated to be 10%. A set-up to measure the longitudinal rms bunch length is available in front of the DTL [13]. It measures the time of impact of a single ion on a foil. This time is related to a 36 MHz master oscillator. The resolution is 0.3° (36 MHz). Prior to the high intensity measurements a scan with very low beam current was done, demonstrating that no emittance growth occurs in absence of space charge forces. Afterwards the HSI was set to obtain 7.1 mA of $^{40}Ar^{10+}$ in front of the DTL. Horizontal and vertical phase space distributions were measured in front of the DTL. The longitudinal rms bunch length was

measured at the entrance to the DTL. The DTL quadrupoles were set to the required zero current transverse phase advance σ_o. Due to space charge the phase advances in all three dimensions were depressed. The transverse depression reached from 14% (130°) to 43% (35°). Afterwards the quadrupoles and re-bunchers preceding the DTL were set to obtain full transmission and to minimize low energy tails of the beam. For each value of σ_o horizontal and vertical beam emittances were measured at the exit of the DTL with a resolution of 0.8 mm in space and 0.5 mrad in angle.

Each emittance measurement delivers a two dimensional matrix of discrete slit-positions and discrete angles. The data are processed by the measurement & evaluation program PROEMI [14]. Simulations deliver a set of six dimensional particle coordinates. This ensemble is projected onto a pixel-grid having the same characteristics as the slit/grid device used for the measurements. The grid is read by the measurement evaluation program PROEMI such that data reduction was done in the same way as for measured data.

INPUT FOR SIMULATIONS

The reconstruction of the initial distribution was done in two steps. First the rms Twiss parameters were determined. In the second step the type of distribution was reconstructed. The transverse rms measurements and the longitudinal rms measurements of the initial distribution, done at different locations along the beam line (Fig. 2) were combined in a self-consistent way based on envelope tracking of an rms equivalent KV-distribution [15]. The reconstruction of the type of distribution is based on evaluation of the brilliance curve, i.e. the fractional rms emittance as a function of the fraction [10]. Different amounts of halo have been found in the two transverse plane. For proper modelling of the initial distribution, both brilliance curves must be reproduced simultaneously. This was achieved by using a distribution function as

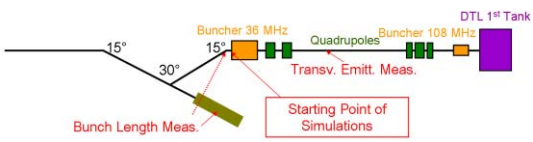

Figure 2: Matching section to the DTL including the reference points used for reconstruction of the initial phase space distribution.

$$f(R) = \frac{a}{2.5 \cdot 10^{-4} + R^{10}}, \quad R \leq 1 \qquad (1)$$

and $f(R) = 0$ for $R > 0$ with

$$R^2 = X^2 + X'^2 + Y^{1.2} + Y'^{1.2} + \Phi^2 + (\delta P/P)^2 , \quad (2)$$

where a is the normalization constant and the constant in the denominator results from the cut off condition at $R = 1$. By defining the radius R using different powers for different sub phase spaces the halos within the planes could be modelled. Since for the longitudinal phase space distribution no measurement but on the rms bunch length is available, a Gaussian distribution cut at 4σ is assumed. This can be approximated by setting the respective powers in the definition of R to a value of 2. It must be mentioned that the applied method is not sensitive for eventual correlations among different planes. Such correlations have been assumed to be zero.

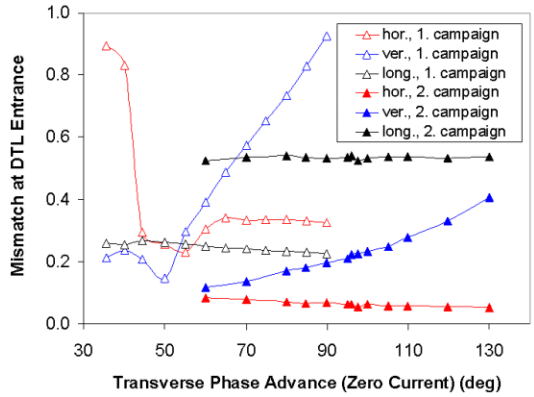

Figure 3: Mismatch between beam rms Twiss parameters and periodic Twiss parameters at injection into the DTL as a function of the phase advance σ_o for the two campaigns.

MEASUREMENTS WITH MODERATE MISMATCH

The reconstructed initial distribution together with the applied setting along the matching section to the DTL was used to estimate the amount of mismatch [16] at the DTL entry using the DYNAMION code. As shown in Fig 3 the mismatch has been very small for intermediate σ_o and moderate in one plane for low and for high values of σ_o. For the applied σ_o from 35° to 90° full beam transmission was observed through the DTL in the experiment. The codes predicted losses of about 2%. Figure 4 displays final horizontal phase space distributions at the DTL exit as obtained from measurements and from simulations for three different values of σ_o. The simulated final distributions look quite similar. Simulations could reproduce the wings attached to the core measured at highest phase advances. But the codes did not show the asymmetric distributions measured at lowest phase advances. The simulated longitudinal phase spaces showed filamentation and emittance growth due to slight rf-bucket overflow at the DTL injection. Final transverse rms emittances are presented in Fig. 5 to Fig. 7 as a function of the transverse phase advance σ_o. The measurements and the simulations revealed lowest emittances at $\sigma_o \approx 60°$. In general good agreement among the codes was found for the sum of the two transverse emittances but codes slightly underestimate the emittance growth. This is reasonable since the codes assume a machine without errors causing additional growth [17]. However, within single planes considerable

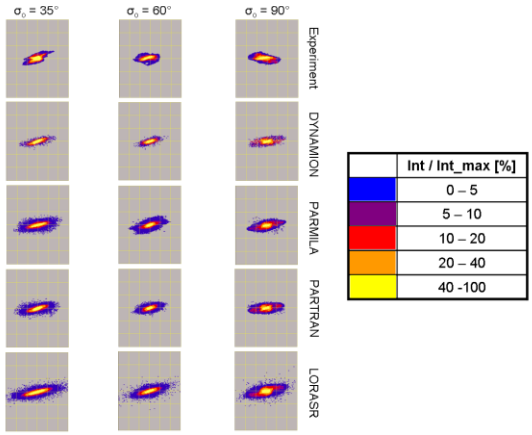

Figure 4: Top to bottom: horizontal phase space distributions at the DTL exit. Left: σ_o = 35°; center: σ_o = 60°; right: σ_o = 90°. The scaling is ± 24 mm (horizontal axis) and ± 24 mrad (vertical axis), respectively.

differences among the codes have been found.

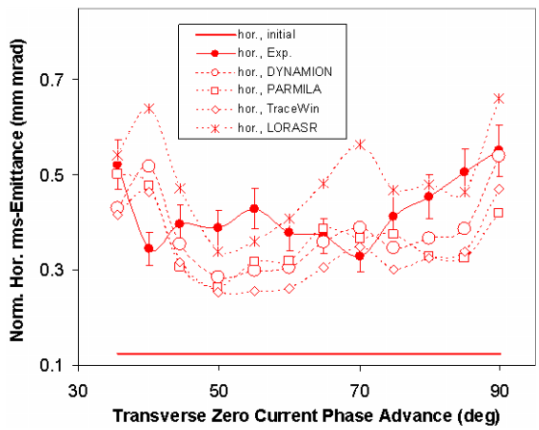

Figure 5: Horizontal rms emittance at the end of the DTL as a function of σ_o.

RMS MATCHED DTL-INJECTION

In order to minimize the mismatch to the DTL a dedicated computer code was created working in two steps. In the first step the periodic solution at the entrance to the DTL is calculated. Acceleration is neglected and the gap voltage and phase are adjusted such that the transverse defocusing is equal to the accelerating case. The DTL starts at a symmetry point of the periodic envelope and accordingly all three α-parameters, i.e. envelope slopes, are assumed to be zero. In the following an iterative procedure as depicted in Fig. 8 is applied. Initial values for the β-functions are used to track the envelope through one period. This is done by numerically solving the coupled system of differential equations from Ref. [15] describing the propagation of the beam's rms envelopes with space charge. As a solver the routine *rkqs* from [18] has been used. The next iteration

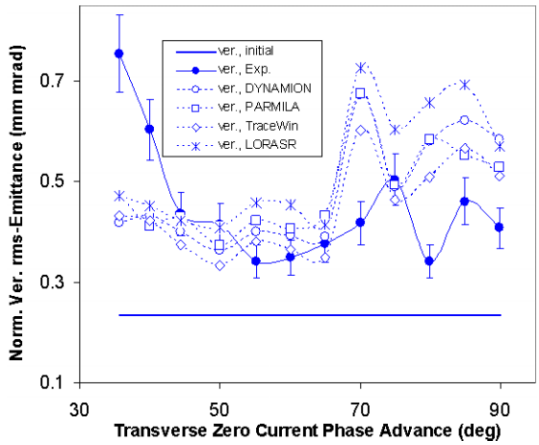

Figure 6: Vertical rms emittance at the end of the DTL as a function of σ_o.

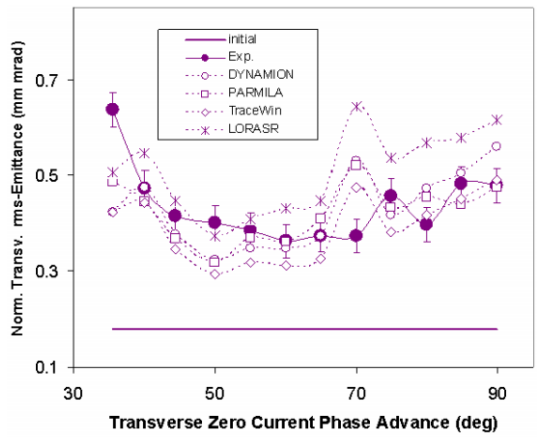

Figure 7: Mean value of horizontal and vertical rms emittance at the end of the DTL as a function of σ_o.

uses the mean of initial and final β-function as starting condition. Convergence is reached in less than 30 iterations. The second step of matching determines the settings of the focusing elements of the matching section (Fig. 2). Using the rms parameters of the reconstructed distribution at the entrance to the section as initial condition for the tracking equations, the final rms parameters at the DTL entrance depend on the focusing strengths f_i of the two bunchers and the five quadrupoles of the section. The final rms parameters together with the periodic solution define the mismatch M_i in each plane [16]. Matched injection is achieved if M is zero in each of the three planes. Defining

$$F(f_1 \ldots f_7) = M_x^3(\ldots) + M_y^3(\ldots) + M_z^3(\ldots) \quad (3)$$

as a function of the seven focusing strengths in the matching section, the matching is optimized for the setting $f_1 \ldots f_7$ that minimizes F. Minimization of F is done with the routine *powell* from [19]. It turned out that the sum of the third powers gives the best results w.r.t. convergence and final mismatch. During all experiments $M_i = 0$ has been reached within less than three minutes.

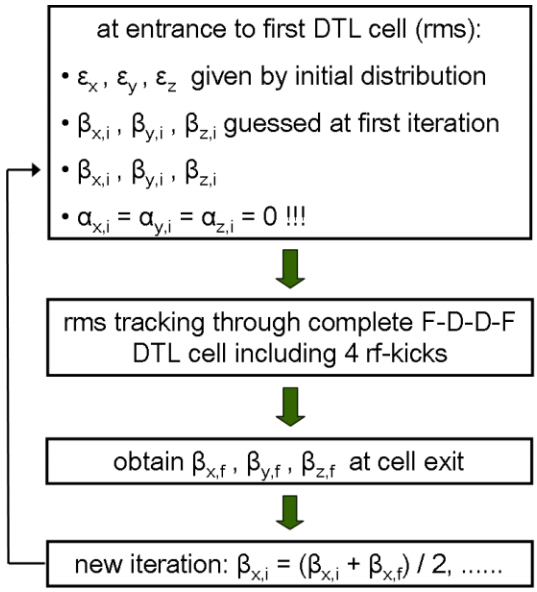

Figure 8: Flux diagram to obtain the periodic solution of the beam envelope inside the periodic DTL.

The emittance growth scan was repeated with matched injection by re-measuring rms emittance growth rates at three different phase advances. It was demonstrated that the application of the matching routine reduced the emittance growth significantly. Fig. 9 plots the measured growth rates as well as results from simulations using the DYNAMION code. In addition to reduced growth, matching leads to

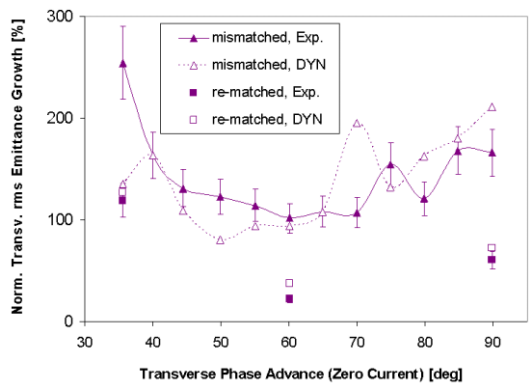

Figure 9: Relative growth of mean value of horizontal and vertical rms emittance at the end of the DTL as a function of σ_o. Data are shown for moderate mismatch and for the case of minimized mismatch.

an improved agreement between measurements and simulations. In order to further investigate this correlation all recent UNILAC experiments were evaluated w.r.t. accuracy of code predictions as a function of mismatch. The agreement improves with the quality of the matching to the DTL. This is plotted in Fig. 10, where the relative deviation between the measured emittances and the code predictions is plotted versus the mean transverse mismatch. For a

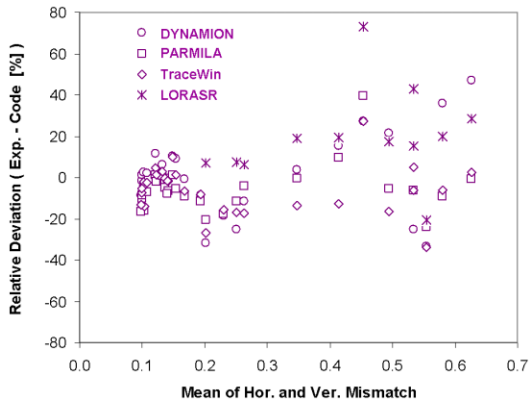

Figure 10: Relative deviation between final transverse rms emittances as measured and predicted by the codes versus the mean of horizontal and vertical mismatch to the DTL.

mean mismatch of less then 20% the codes accuracies are always better than 20%, while for larger mismatches the codes might deliver final rms emittances that differ of up to 80% from the experimental values.

OCTUPOLAR RESONANCE IN A LINAC

The parabolic term of the space charge density rises a field term of third order, i.e. a octupolar term. Since matched beam envelopes perform quasi-periodic oscillations, this term acts as a periodic third-order perturbation. The perturbation is resonant if the envelope phase advance per period, i.e. 360°, is four times higher than the single particles phase advance. Accordingly, a resonance is expected to occur at a depressed transverse phase advance of 90°. Simulations using the PARMILA and DYNAMION codes suggested to perform the measurement at the UNILAC [11]. To exclude any inter-tank mismatch along the DTL just the first tank was used and the zero current phase advance σ_o was varied from 60° to 130°. A characteristic feature of this resonance is the formation of four wings in the transverse phase space distributions being attached to the beam core.

Measured and simulated transverse phase space distributions at the tank exit are plotted in Fig. 11, as well as the corresponding rms emittances. Distributions corresponding to phase advances far away from the resonance have elliptical shapes. At $\sigma_o \approx 100°$, i.e. at a depressed phase advance of 90°, instead the measurements and the simulations clearly revealed four arms, which are typical for a resonant octupolar interaction. A detailed description of the campaign on the octupolar resonance can by found in [11, 12] pointing out that the observed emittance growth is not caused by the well-known envelope instability but by the octupolar space charge potential term.

We summarize that the codes are reliable tools for machine optimization and for the preparation of beam experiments. However, qualitative accuracy strongly depends on the quality of beam matching. Good matching is re-

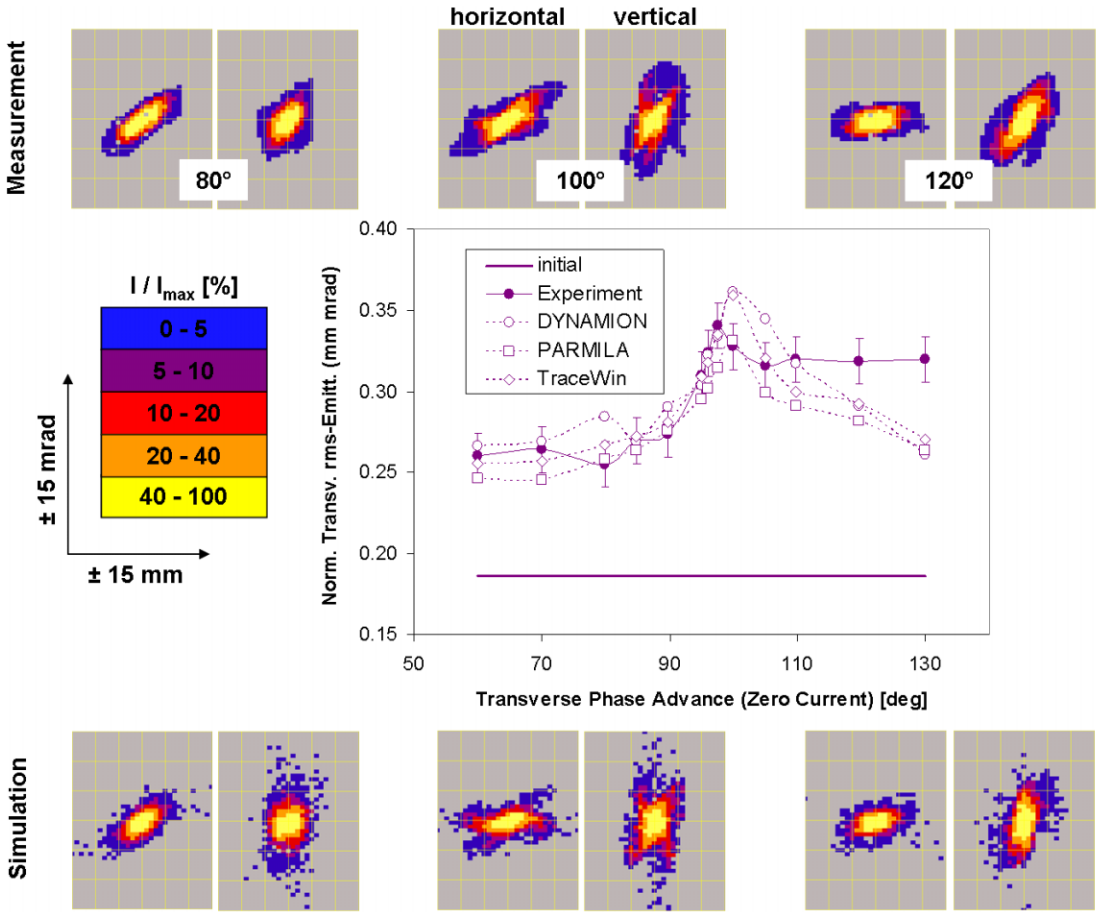

Figure 11: Upper and lower: phase space distributions at the exit of the first DTL tank as obtained from measurements and from the DYNAMION code for phase advances σ_o of 80°, 100°, and 120°. Left (right) side distributions refer the horizontal (vertical) plane. The scale is ±15 mm and ±15 mrad. Fractional intensities refer to the phase space element including the highest intensity. Center: Mean of horizontal and vertical normalized rms emittance behind the first DTL tank as a function of σ_o.

quired for useful predictions on the sum of transverse emittances. Considerable deviations within single planes were observed also for well matched beams.

REFERENCES

[1] R. Ryne et al., Proc. of the HB2008 Workshop, Nashville, U.S.A. (2008).

[2] S. Nath et al., Proc. of the 2001 Part. Accel. Conf., Chicago, U.S.A., (2001).

[3] A. Franchi et al., Proc. of the XXIII Linac Conf., Knoxville, U.S.A., (2006).

[4] A. Franchi et al., http://www-dapnia.cea.fr/Phocea/file.php ?class=std&&file=Doc/Care/note-2006-011-HIPPI.pdf

[5] W. Barth et al., Proc. of the XXII Linac Conf., Lübeck, Germany, (2004).

[6] S. Yaramyshev et al., Nucl. Instrum. Methods Phys. Res., A **558**, 90 (2006).

[7] J.H. Billen and H. Takeda, PARMILA Manual, Report LAUR-98-4478, Los Alamos, 1998 (Revised 2004).

[8] http://irfu.cea.fr/Sacm/logiciels/index.php.

[9] R. Tiede, PhD thesis, Goethe University Frankfurt a.M., to be published.

[10] L. Groening et al., Phys. Rev. ST Accel. Beams **11**, 094201 (2008).

[11] D. Jeon et al., Phys. Rev. ST Accel. Beams **12**, 054204 (2009).

[12] L. Groening et al., Phys. Rev. Lett. **102**, 234801 (2009).

[13] P. Forck et al., Proc. of the XX Linac Conf., Monterey, U.S.A., (2000).

[14] G. Riehl, *PROEMI: An emittance measurement and evaluation code*. The manual is available from the code author on request (g.riehl@gsi.de).

[15] T.P. Wangler, "Rf Linear Accelerators", John Wiley & Sons Inc., New York, p. 278, (1998).

[16] see Ref. [15], p. 217.

[17] K.R. Crandall, AOT Division Technical Note LA-CP-96-16, January 22, 1966.

[18] W.H. Press et al., "Numerical Recipies in C", Cambridge University Press, Cambridge, p. 719, (1992).

[19] see Ref. [18], p. 419.